IEEE Access
Multidisciplinary | Rapid Review | Open Access Journal

Received March 7, 2020, accepted March 19, 2020, date of publication March 24, 2020, date of current version April 8, 2020.

Digital Object Identifier 10.1109/ACCESS.2020.2983062

Bandwidth Enhanced Circularly Polarized Fabry–Perot Cavity Antenna Using Metal Strips

YANG CHENG, (Student Member, IEEE), AND YUANDAN DONG, (Senior Member, IEEE)
School of Electronic Science and Engineering, University of Electronic Science and Technology of China, Chengdu 611731, China
Corresponding author: Yuandan Dong (ydong@uestc.edu.cn)

ABSTRACT This paper introduces a novel single feed wideband Tai Chi-shaped circularly polarized (CP) antenna that utilizes a Fabry-Perot cavity (FPC) with a 3D printed structure to increase the antenna gain and axial ratio (AR) bandwidth. Besides, a novel method is proposed for AR bandwidth enhancement. Some simple metal strips are introduced, which could adjust the phase of the particular electric field component. By placing the metal strips at an optimal position, the AR bandwidth of the antenna could be effectively broadened. Note that this method has little effect on the other antenna performance and it does not require additional structural changes. The proposed method to increase the axial ratio bandwidth is very simple and effective. The Tai Chi-shaped antenna consists of two separate small patches and two suspended metal rods. The two small patches are 180° out-of-phase excited which are centro-symmetrically placed to form a larger and complete circular patch. The two small patches and the total split patch generate two minimum AR points, which substantially broadens the AR bandwidth. Adding two layers of FR4 substrate to the antenna constitutes an FPC, and the antenna peak gain is increased from 9.42 dBic to 14.44 dBic. In addition, the AR bandwidth has been increased from 27.73% to 44.42%. In order to further increase the AR bandwidth of the CP antenna, some simple metal strips have been added to the FPC substrate. The AR bandwidth has been enhanced from 44.42% to 53.46% (4.07 - 7.04 GHz). Compared with other CP antennas with FPC, our proposed antenna shows advantages in terms of substantially broadened impedance and AR bandwidth, high gain, and low fabrication cost.

INDEX TERMS Axial ratio (AR), circular polarization, Fabry-Perot Cavity (FPC) antenna, metal strips, wideband.

I. INTRODUCTION

Fabry-Perot Cavity antenna (FPCA) [1] has received increasing attention in recent years because it has superior advantages in terms of simple structure, small size and high gain compared with traditional antennas such as lens antennas [2], reflector antennas [3], leaky-wave antenna [4] and antenna arrays [5] (e.g. microstrip antenna arrays). Circularly polarized (CP) antennas are a type of antennas with axial ratio (AR) typically lower than 3 dB. Due to the features of circular polarization, CP antennas have several important advantages compared to antennas with linear polarization, such as combating multi-path interferences or fading [6]; reducing the ''Faraday rotation'' effect [7], and no strict orientation requirement between transmitting and receiving antennas.

Recently, in order to combine the advantages of CP antennas and FPCAs, a lot of designs have been proposed and developed for CP FPCAs [8]–[13]. These antennas are basically composed of three parts: an excitation source, a total reflection ground and a partially reflective surface (PRs). The excitation source may be a CP antenna, and the Fabry-Perot cavity (FPC) provides the effect of gain enhancement or maybe a linearly polarized antenna, and the realization of CP is achieved by exploiting the polarization-dependent characteristic of the cavity. In order to realize broadband and high-gain CP FPCAs, most of the designs utilize wide-band circularly polarized antennas as the excitation source, which are able to enhance the antenna gain but not the circular polarization (or AR) bandwidth. In [8] a chamfered slotted patch

The associate editor coordinating the review of this manuscript and approving it for publication was Davide Comite.

antenna is used as the CP excitation source. Sequentially rotated feeding technology was used in [14] to increase the circular polarization bandwidth, resulting in a 3 dB AR bandwidth of 17% and a maximum gain of 14.1 dBic. An FPCA with a metamaterial-loaded cavity is proposed in [9], where an overlapped impedance and AR bandwidth of 6.7% (from 9.6 to 10.27 GHz) was realized. In [10] a wideband CP magneto-electric dipole antenna (CP MEDA) was used as an excitation source. It employs a partially reflecting surface made by a substrate with arrays of metal patches printed on both the top and bottom sides to improve the antenna gain. The 3 dB AR bandwidth is about 29.3% (12.4-16.8 GHz) and the maximum CP gain is 11.45 dBic. A compact wideband CP FPCA using a resonating structure made of thin dielectric slabs is proposed in [11] achieving a 3 dB AR bandwidth of 47.7% (5.9-9.6 GHz) and 3dB gain bandwidth of 50.9% (5.7-9.6 GHz). However, the excitation source in [11] is a CP crossed dipole antenna, and the original 3dB AR bandwidth of the excitation source is 36.68%. The overall AR bandwidth improvement is not very significant.

In this paper, a 3D printed Tai Chi-shaped wideband circularly polarized antenna that uses a two-layer conventional Fabry-Perot cavity (FPC) structure to increase the gain and axial ratio (AR) bandwidth of the antenna. In order to achieve a significant enhancement in the CP bandwidth, some metal strips are added to double-layer FPC. The phase difference between the two orthogonal electric field components of the antenna is optimized, thereby resulting in a wider CP bandwidth. The increase in the AR bandwidth is very obvious. Note that this method has little effect on other performance of the antenna and it does not require additional changes to the antenna. This method provides a new idea for improving the AR bandwidth of CP FPCA. The AR bandwidth of the original Tai Chi shaped patch antenna is 27.73%, and the AR bandwidth of final CP FPCA with metal strips is 53.46%. The maximum gain of the antenna is increased from 9.42 to 14.44 dBic.

This paper is organized as follows: the antenna configuration, CP principle and the measured results of the normal CP FPCA without metal strips are elaborated in Section II. The improvement approach and the final antenna configuration, including all the simulated and measured results are illustrated in Section III. The proposed antenna is compared with the previous work. Finally, a conclusion expatiates in section IV.

II. TWO LAYER CP FPC ANTENNA WITHOUT STRIPS

A. ANTENNA CONFIGURATION

The geometry and configuration of the proposed 3D CP FPCA without metal strips are shown in Fig. 1. The excitation source of FPC is a CP patch antenna of Tai Chi shape, as shown in Fig. 1(b). There are two suspended metal rods in the Yin and Yang sides of the Tai Chi patch to feed the antenna. The feeding is coupled by a microstrip line through the slot to two suspended metal rods and then excite the two separate patches with a phase difference of 180 degrees as shown in Fig. 1(d). The patch antenna source is etched on the low cost F4BME220 substrate with a relative permittivity of 2.2, a thickness of 1 mm and a loss tangent of 0.0009.

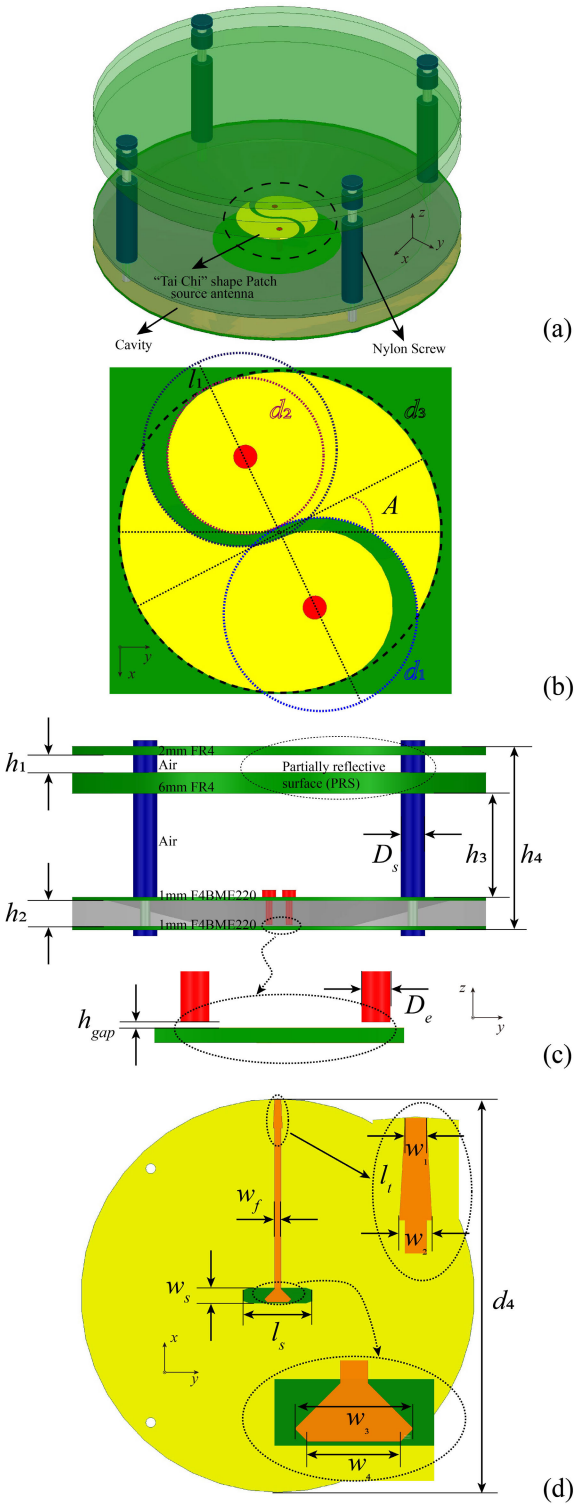

FIGURE 1. Configuration of the proposed CP FPCA without metal strips. (a) 3D view of the proposed antenna. (b) Top view of Tai Chi shaped circularly polarized patch antenna. (c) Cross-sectional view of the antenna. (d) Bottom view of the antenna.

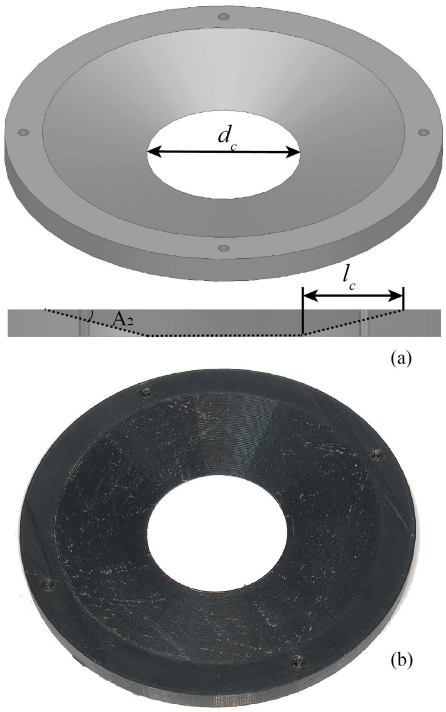

FIGURE 2. 3D printed cavity. (a) 3D simulation model. (b) Prototype of 3D printed cavity (without copper).

TABLE 1. Dimensions of the proposed antenna (Unit: mm/deg).

Parameter	l_1	d_1	d_2	d_3	A	h_1	l_t	d_c
Value	1	8	6.5	13.37	25.3	5	8.9	41.88
Parameter	h_2	h_3	h_4	D_s	D_e	h_{gap}	l_s	l_c
Value	7.405	30	53.07	3.5	2	0.43	20.99	28.57
Parameter	w_f	w_1	w_2	w_s	w_3	w_4	d_4	A_2
Value	1.9	1.9	2.84	4.57	8	6.38	120	15

In order to increase the bandwidth of the source antenna, a thick air substrate is used to reduce the Q value of the antenna. A 3D printed metalized cavity is added to the air medium to support the substrate of the antenna while also improving the CP bandwidth and gain. The geometry of the cavity is shown in Fig. 2. In order to reduce the cost and processing difficulty, 3D printing technology was used to fabricate the three-dimensional plastic structure. Then a layer of copper tape was used to wrap the structure instead of using the solid metal cavity. The substrate used for the PRS is FR4 with a relative dielectric constant of 4.4 and a loss tangent of 0.02. The thickness of the two FR4 substrates is 2 mm and 6 mm, respectively, as shown in Fig. 1(c). The 6 mm thick FR4 substrate consists of three layers of 2 mm thick substrate. The detailed parameters of the antenna structure are shown in Table 1. The fabricated antenna is presented in Fig. 3.

The structure and dimensions of the proposed bidirectional antenna are shown in Fig. 2 and Table. 1. This antenna consists of two curved slots etched on the bottom layer of the PCB. The slot is obtained by cutting a bigger ellipse with a smaller rotated ellipse. Additionally, we cut its edge with

TABLE 2. Dimensions of the proposed antenna (Unit:mm/deg).

Parameter	l_2	l_3	l_4	l_5	l_6	w_5	w_6
Value	30	27.65	5	4.57	1.78	4	6
Parameter	w_7	w_8	w_9	w_{10}	w_{11}	A_s	
Value	5	1.9	3	6.4	7.2	25	

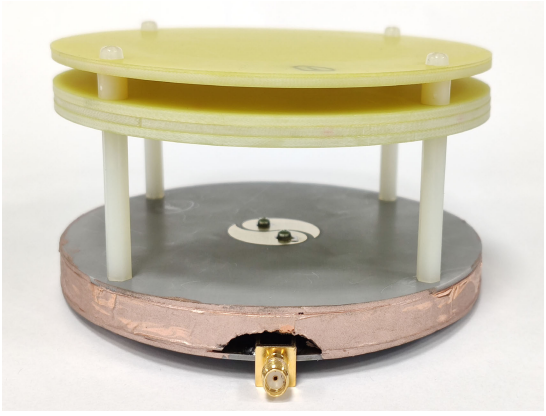

FIGURE 3. A photograph of the proposed antennas.

a straight line to leave more space to the ground plane. The lowest end of two ellipses coincides with the center of the antenna, and the smaller ellipse is clockwise rotated along its lowest end by θ_2. To leave a gap of reasonable width at the junction of the two slots, a tiny rectangular slot with a width of 1 mm and a rotated angle of $\theta_2/2$ is placed at the center of the bottom layer.

B. DESIGN PRINCIPLE OF THE PROPOSED ANTENNA

The proposed Tai Chi source antenna consists of two ''fish'' shaped patches, each of which is fed by a suspended metal rod. The ''fish'' shaped patches are out-of-phase excited due to the use of aperture (slot) coupled microstrip feeding line. The two edges of the slot have opposite voltage. It is well-known that most of the single-feed CP microstrip antennas require a perturbation on the structure from two orthogonal modes. The ''fish'' shaped patch can be considered as a capacitor loaded the small patch. Two orthogonal modes could be excited as explained by the field distribution shown in Fig. 4. A large Tai Chi shaped patch antenna is formed by combining these two ''semi-circular'' patches, which are centro symmetrically placed and 180° out-of-phase excited. It broadens the impedance bandwidth and generates the other minimum AR point. Two CP resonance points are observed on the AR curve as shown in Fig. 5. The simulated $|S_{11}|$ and peak gain are also presented in Fig. 5. Fig. 6 displays the simulated radiation patterns of the source antenna at 4.5 and 5.5 GHz. Simulated results show a peak gain of 9.42 dBic and an AR bandwidth of 27.73%. Note that the antenna without FPC height is only 7.405 mm (0.123λ at 5 GHz).

In order to achieve a higher gain, the FPC is designed and introduced. The PRS can be considered as a three-layer structure, consisting of two layers of FR4 and a layer of air. The structure of the Fabry-Perot resonant cavity antenna is so

TABLE 3. Performance comparison of circularly polarized fabry-perot cavity antenna.

Ref.	Overall size (λ_{fmin}*)	Frequency Band	Substrate of FPC	Height of FPC	RLB	Source Antenna Type	SA ARB	CP FPCA ARB	PG(dBic)
[7]	1.58*1.58*0.7	28GHz	Rogers 6010	7.1mm	27.6%	Truncated patch with slot	4.3%	17%	14.2
[8]	3.125*3.125*1.15	10GHz	3D printed	35.3mm	10%	Patch	N.A.	6.7%	14.1
[9]	1.75*1.75*0.775	14GHz	Rogers 5880	12.5mm	54%	CP ME-dipole	N.A.	29.3%	11.45
[10]	1.2*1.2*0.6	8GHz	Rogers 6010	32.54mm	55.7%	Crossed dipole	36.7%	47.7%	15
[11]	2.83*3.23*0.49	6GHz	FR4	22.59mm	>11.6%	Patch	N.A.	>11.6%	17.4
Proposed CP FPCA	**1.6*1.6*0.7**	**5GHz**	**FR4**	**44.67mm**	**48.9%**	**Tai chi-Shaped Patch with suspended screw**	**27.7%**	**40.16%**	**14.8**
With Metal Strips	**1.53*1.53*0.68**				**55.14%**		**27.7%**	**53.46%**	**14.5**

RLB:10-dB return loss bandwidth. SA ARB: source antenna 3-dB axial ratio bandwidth. ARB: 3-dB axial ratio bandwidth
PG: Peak gain.
*λ_{fmin} refers to the free-space wavelength at the lowest operating frequency

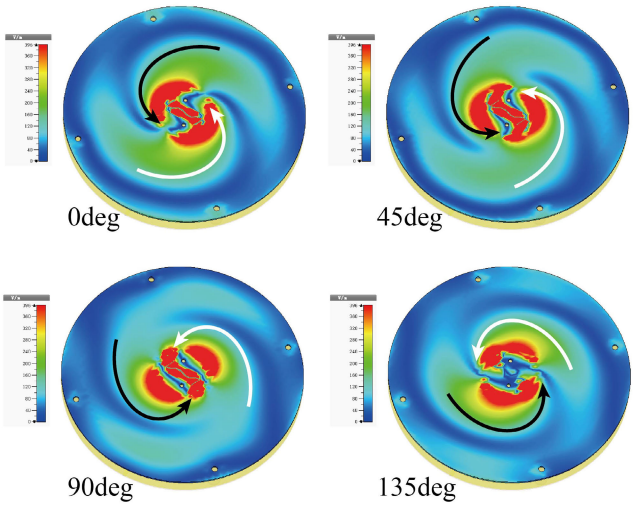

FIGURE 4. The E-field variations for different phase values seen from +z-direction of the antenna.

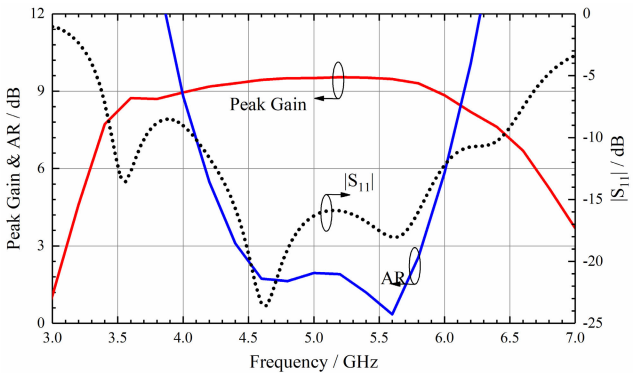

FIGURE 5. Simulated $|S_{11}|$, peak gain, and AR of the Tai Chi-shaped antenna.

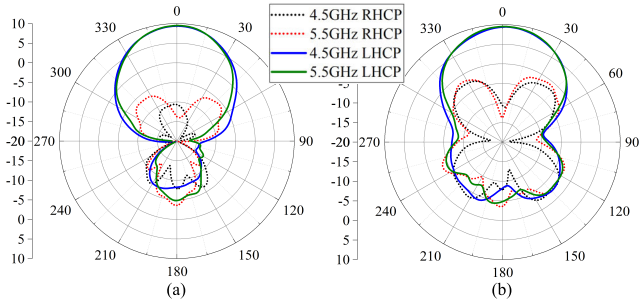

FIGURE 6. Simulated radiation patterns for the Tai Chi–shaped antenna. (a) Phi = 90deg, (b) Phi = 0deg.

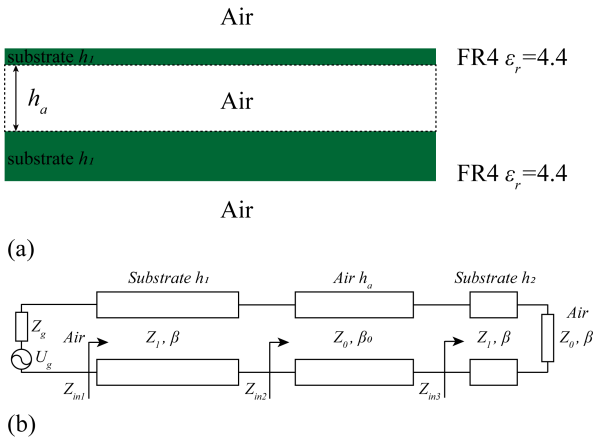

FIGURE 7. (a) The PRS consisting of two FR4 substrates separated by an air-gap and (b) its equivalent transmission line model.

complex that it is difficult to analyze in detail through simple electromagnetic theory and mathematical method. Based on different starting or focusing points, the researchers have put forward a variety of simplified theoretical models and their corresponding analysis methods, such as transverse equivalent network model [15], ray-tracing model [16], leaky-wave model [17] and transmission line model [18].

In this paper, the working principle of the Fabry-Perot resonant cavity antenna is briefly and qualitatively analyzed by means of the transmission line model. The equivalent model of the transmission line for FPC is shown in Fig. 7. The calculation of the transmission line model is completed in the

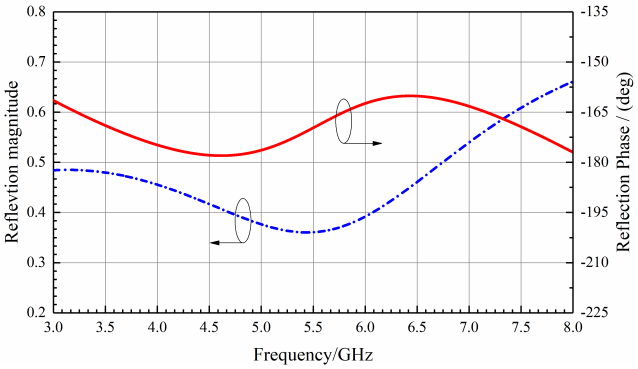

FIGURE 8. Reflection characteristics of the proposed PRS (caculated in advanced design system).

Advanced design system (ADS). Reflection characteristics of the proposed PRS are shown in Fig. 8, where Z_0 and Z_g are the wave impedance in free space, and Z_1 is the wave impedance in the FR4 medium. The calculation formula is as bellow:

$$Z_g = Z_0 = 377\Omega$$
$$Z_1 = \frac{Z_0}{\sqrt{\varepsilon_r}} \tag{1}$$

The reflection phase of FPC resonance needs to satisfy the following condition:

$$\varphi = \frac{4\pi h}{c} f - (2N-1)\pi, \quad N = 0, \pm 1 \ldots \tag{2}$$

where h is the height from the source antenna to PRS, c is the speed of light in vacuum, and f is the frequency. The height of the FPC antenna is determined by the resonance frequency and the reflection phase of the PRS. We can improve the FPC bandwidth in two ways [19]: making the reflection phase of the PRS decrease slowly as the frequency increases, or 2) increasing the phase gradually while increasing the frequency. In this paper, we use the multi-layer dielectric plate structure as the PRS to realize the positive phase gradient, as shown in Fig. 8. Within 4 to 7 GHz frequency range, the reflection phase and magnitude can be maintained in a reasonable range, so that the performance of the FPC can be kept stable in a wide bandwidth. As shown in Fig. 9, the effect of FPC is very obvious. The electric field distribution is more uniform on the PRS, and the gain in the far-field becomes higher. Fig. 10 shows the effect of h_1 on the peak gain and axial ratio of the antenna. The effect of h_3 on the peak gain and axial ratio of the antenna is presented in Fig. 11. h_3 is about half wavelength of the center frequency and a fine-tuned h_1 can improve the antenna performance.

C. SIMULATED AND MEASURED RESULTS

Based on the design principle and analysis mentioned above, an antenna prototype shown in Fig. 3. is fabricated and measured. Fig. 12 shows that the measured impedance bandwidth for return loss less than 10 dB is about 48.9% (3.9-6.43 GHz). Compared with the simulated data, the measured radiation band shifts to a little lower band. The radiation patterns of the fabricated antenna for simulation and measurement at

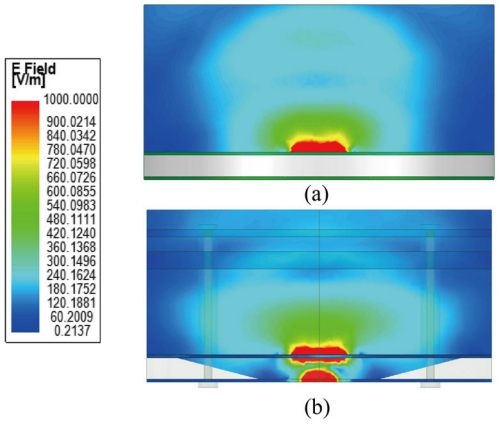

FIGURE 9. Simulated E-field distributions of the antenna (a) without and (b) with the PRS.

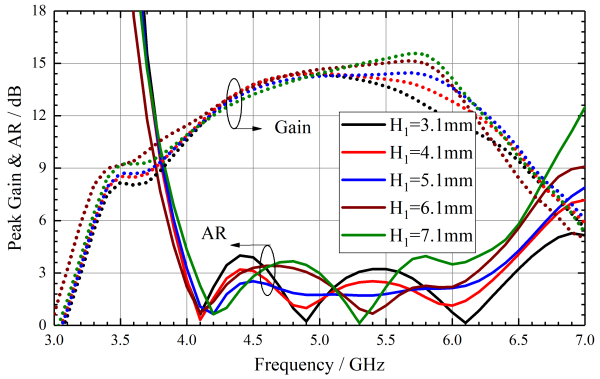

FIGURE 10. Effect of h1 on peak gain and axial ratio of antenna.

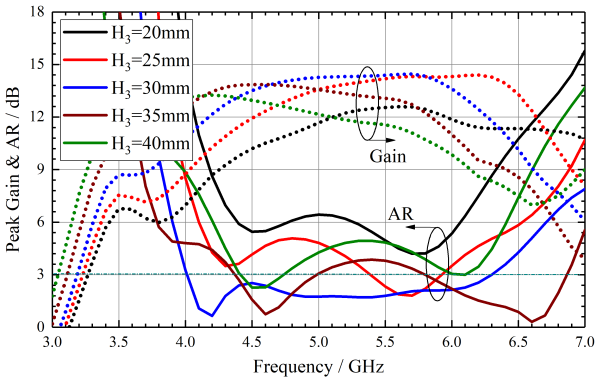

FIGURE 11. Effect of h3 on peak gain and axial ratio of antenna.

different frequencies are illustrated in Fig. 13. Due to the limitations of the measured conditions, the antenna patterns have only been evaluated for the range of −90 to 90 deg. The measured patterns are in good agreement with the simulated data. The small discrepancy is mainly due to the slightly different position of the antenna during the measurement. The measured 3-dB AR bandwidth is more than 40.16% (4-6.01 GHz), as presented in Fig. 14. The measured 3-dB gain bandwidth reaches 40%, from 4.2 GHz to 6.3 GHz with

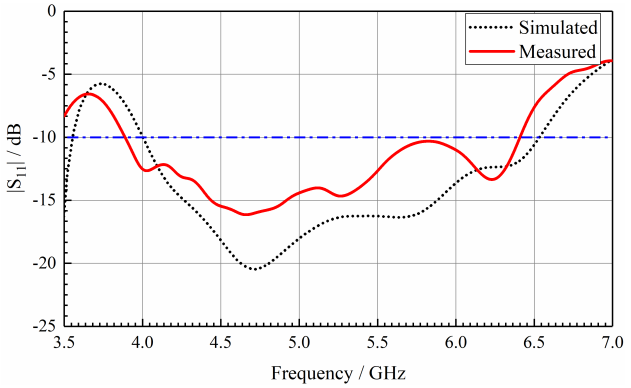

FIGURE 12. Measured and simulated reflection coefficients of the CP FPCA without the metal strips.

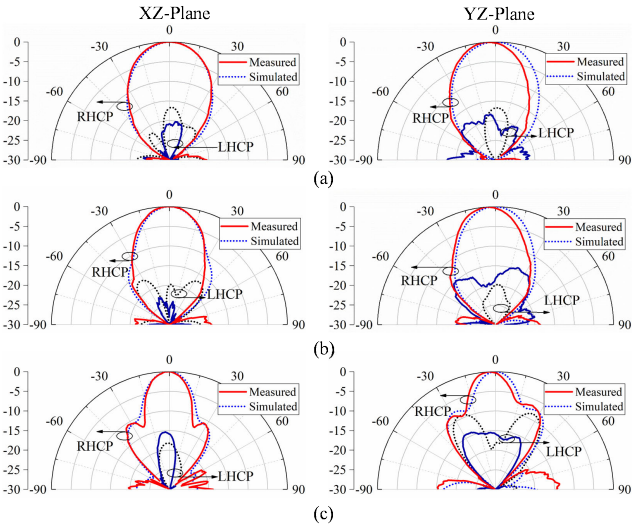

FIGURE 13. Radiation patterns of the proposed CP FPCA without metal strips at (a) 4; (b) 5; and (c) 6 GHz.

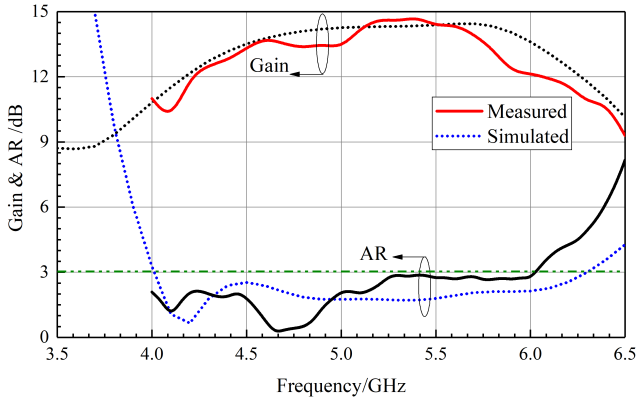

FIGURE 14. Measured and simulated the peak gain and the AR (Phi = 0 deg, Theta = 0deg) of the proposed CP FPCA without the metal strips.

a peak gain of approximately 14.8 dBic (see Fig. 14). Due to some processing and assembling errors, the overall bandwidth of the antenna is slightly shifted to the lower frequency. Although the 3 dB AR bandwidth is not fully determined at the lower frequency side, the overall performance has been fully demonstrated.

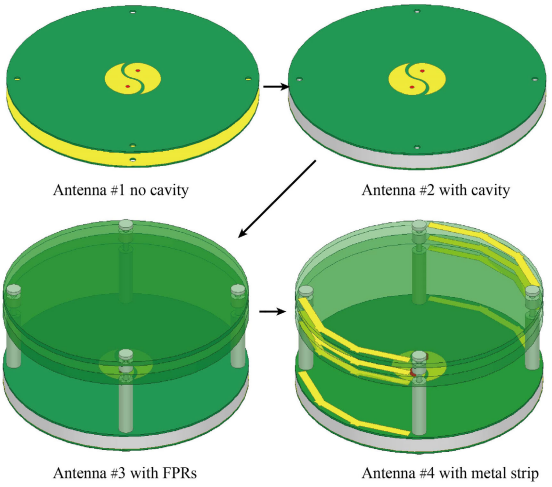

FIGURE 15. Step by step improvement procedures for the antenna structure.

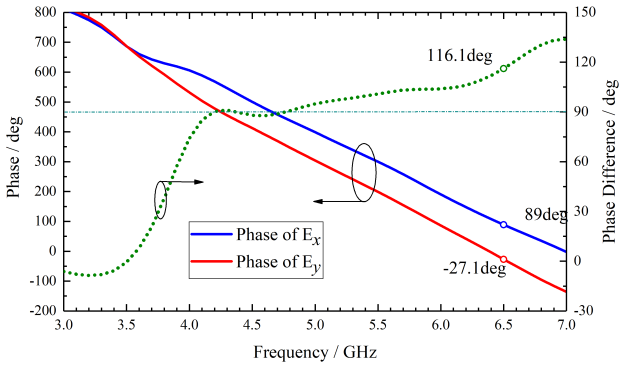

FIGURE 16. Phase and their difference between Ex and Ey without the metal strips.

III. CP FPCA WITH METAL STRIPS

A. ANALYSIS OF THE ANTENNA WITH THE METAL STRIPS

It is well known that CP can be achieved if the total electric field has two orthogonal components which have the same magnitudes and a 90 deg phase difference between the two components [20]. Therefore, the method of widening the CP bandwidth of the antenna is to minimize the amplitude difference of the far-field radiation wave of the antenna as much as possible, and the phase difference should be close to 90 degrees as much as possible.

To further increase the CP bandwidth of the CP FPCA, some metal strips are added on the edges of the PRS. The basic steps for optimizing the antenna performance are summarized in Fig. 15. The reason that adding some metal strips could improve the AR bandwidth of the CP FPCA is that the phase difference between the two orthogonal electric-fields components is adjusted to better maintain 90 deg in a wider frequency range. As shown in Fig. 16 and Fig 19(a), the amplitudes of the two E-field components are almost the same. Therefore, the cause of the AR deterioration at 6.5 GHz is that the phase difference between the two orthogonal E-field components is too large (116.1 deg). As well known,

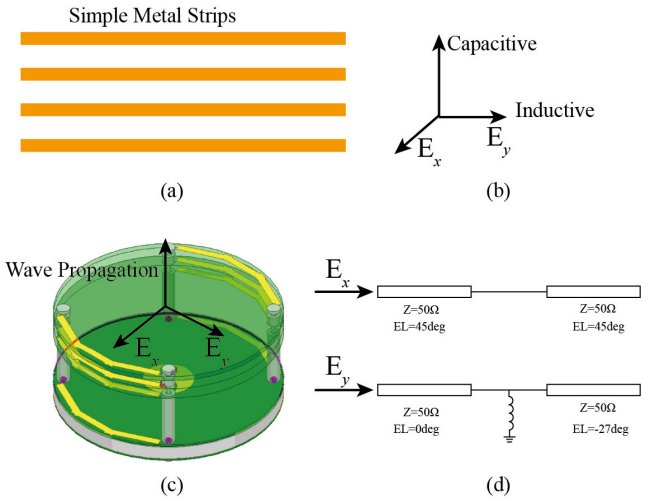

FIGURE 17. An explanation for the inductive and capacitive metal strips. (a) Simple metal strips model. (b) The relationship between the E- field direction and the capacitance or inductance for the metal strips. (c) Two orthogonal E-field directions for the proposed antenna. (d) The equivalent circuit models for the two orthogonal E-field components during propagation.

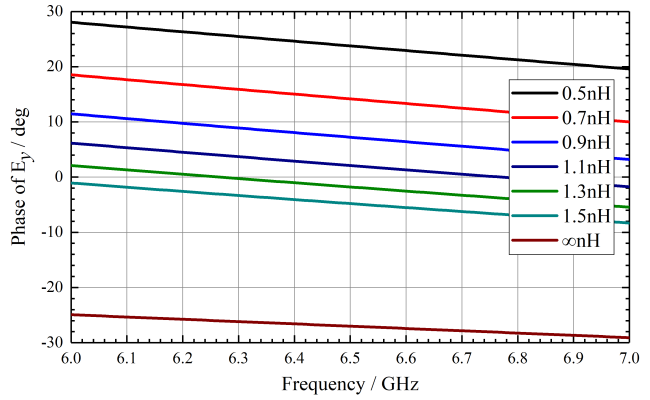

FIGURE 18. The phase relationship for Ey by changing the inductance.

the simple metal strips act as a shunt inductance for E-field components along the strips and as a shunt capacitance for E-field components perpendicular to the strips [21], [22]. Fig. 17 shows the two orthogonal E-field components for the proposed antenna and their equivalent circuit models during wave propagation for each orthogonal E-field components. By placing the metal strips on the edge of the FPC, shunt inductance is introduced in the propagation path which improves the phase of Ey. Note that the direction of the metal strips should be parallel to the direction of Ey. We use the ideal transmission lines in the Advanced Design System (ADS) to simulate electromagnetic wave propagation. Fig. 18 shows the relationship between the inductance and phase of Ey. As shown, when a 1.3 nH shunt inductor is introduced, a wideband 90 deg difference between the two orthogonal E-field components could be realized.

In order to compare the effects of the 3D printed cavity, FPC, and metal strips on performance, the amplitude difference and phase difference of the two orthogonal electric field

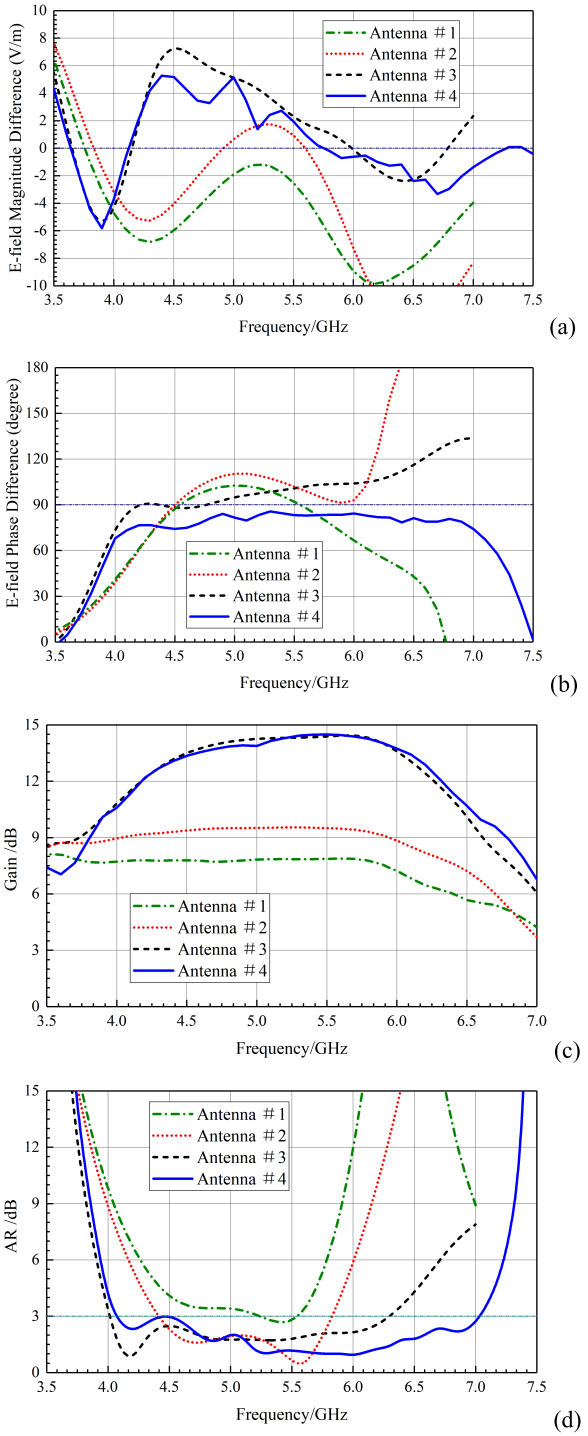

FIGURE 19. (a) Amplitude and (b) phase difference between E-field components in the antenna far field, (c) Peak gain and (d) AR of the different antennas.

components in the far-field of each antenna is illustrated in Figs. 19(a) and (b). It can be seen from Fig. 19 that the 3D printed cavity mainly plays the role of optimizing the phase difference, while its influence on the amplitude difference is small. This is due to the fact that the volume of the cavity is too small. The gain of the antenna increases by about 1.8 dB (7.8 to 9.6 dBic).

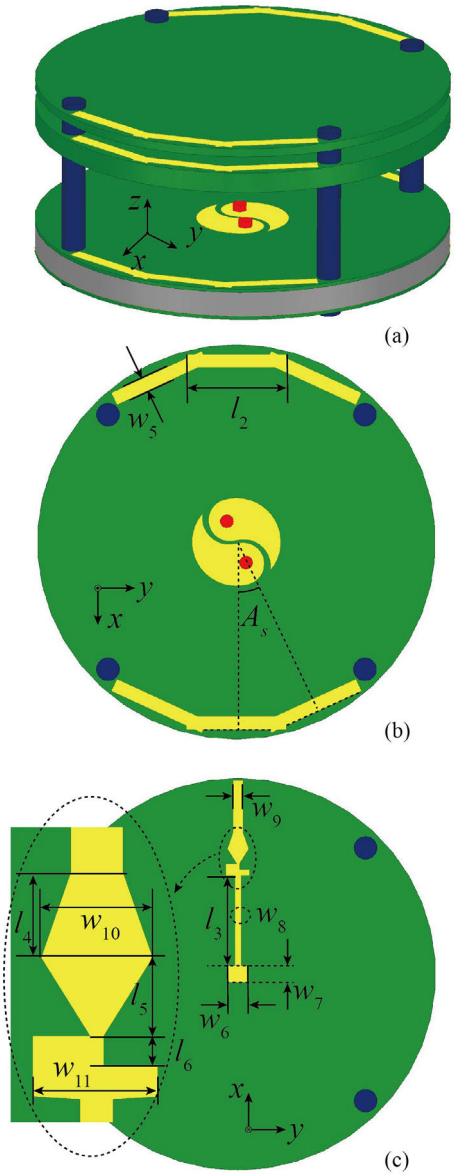

FIGURE 20. Configuration of the proposed CP FPCA with metal strips. (a) 3D view of the proposed antenna. (b) Top view of Tai Chi shaped circularly polarized patch antenna. (c) Bottom view of the antenna.

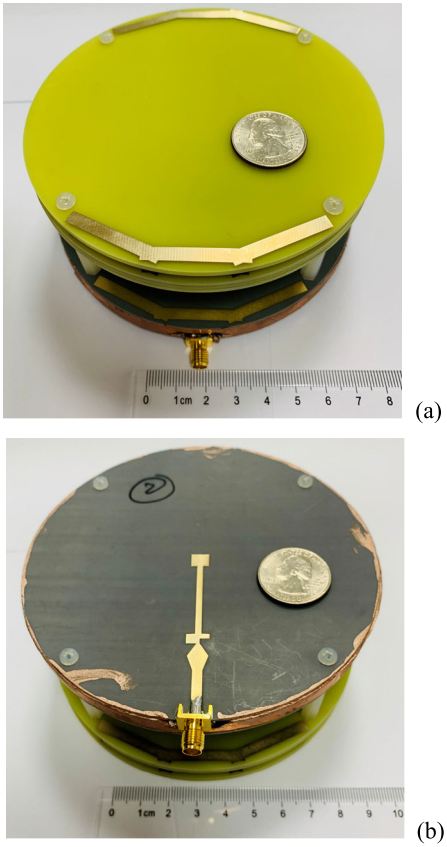

FIGURE 21. Photograph of the fabricated CP FPCA with metal strips. (a) Top view, and (b) bottom view.

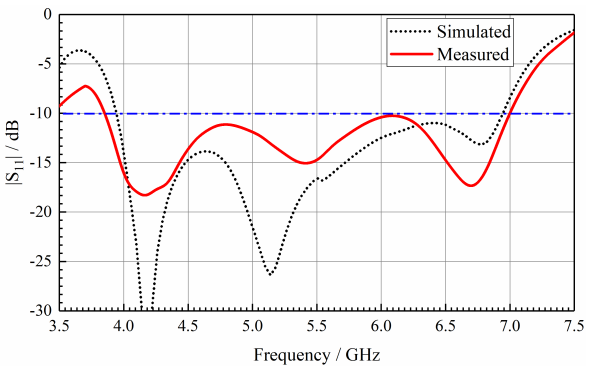

FIGURE 22. Measured and simulated reflection coefficient for the CP FPCA with metal strips.

The FPC not only greatly improves the amplitude difference of the orthogonal E-field components in the far-field, but also optimizes the phase difference. The metal strip is etched at the edge of the FPC with little effect on the far-field gain. However, the metal strip plays an important role in phase regulation. The phase difference of the electric field in the far-field of the antenna maintains a very mild change from 4 to 7 GHz, which greatly widens the CP bandwidth.

In summary, by improving the amplitude difference and phase difference of the two orthogonal far-field E-field components, the CP bandwidth of the antenna is increased from 27.73% (4.41-5.83GHz) to 53.46% (4.07-7.04GHz). In addition, the 3D printed cavity together with the FPC also increases the antenna gain from 7.8 to 14.8 dBic.

B. ANTENNA CONFIGURATION

Fig. 20 shows the geometry of the proposed CP FPCA with metal strips. The basic structure of the antenna is the same as that of the CP FPCA mentioned above, except that the metal strips are printed on the edge of the substrate of the FPC and the antenna. The CP bandwidth of the antenna exceeds the impedance bandwidth, so some matching branches and gradient lines are added to the feed line to improve the impedance matching. A photograph of the fabricated CP FPCA with metal strips is illustrated in Fig. 21.

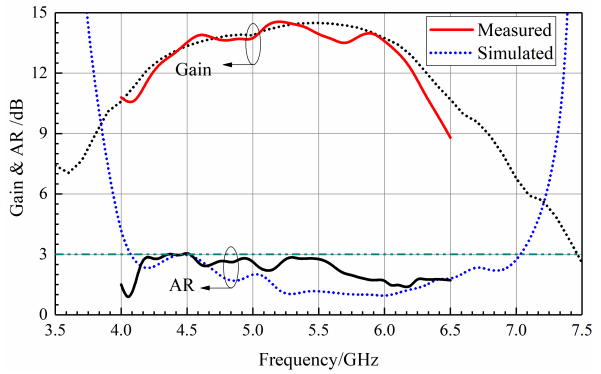

FIGURE 23. Measured and simulated peak gain and the AR (Phi = 0 deg, Theta = 0 deg) of the proposed CP FPCA with metal strips.

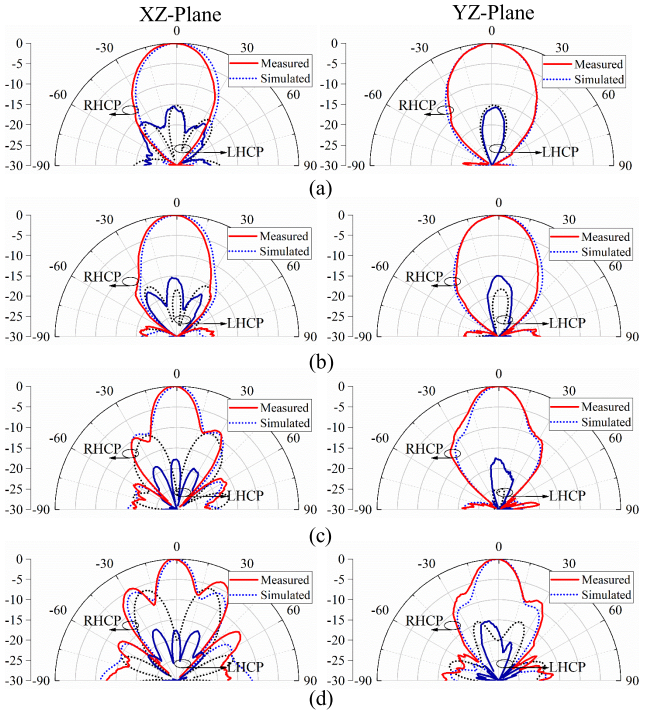

FIGURE 24. Radiation patterns for the proposed CP FPCA with metal strips at (a) 4GHz, (b) 5GHz, (c) 6GHz, (d) 6.5GHz.

C. SIMULATED AND MEASURED RESULTS

The measured S-parameters from 3.5 to 7.5 GHz are shown in Fig. 22, compared with the simulated results. The measured results are basically consistent with the simulation. The impedance bandwidth is increased from the previous 48.05%(4-6.53GHz) to 55.14% (3.82-7.01GHz) due to matching stubs. The radiation patterns were measured in a far-field chamber. Due to the limitations of the test system, the radiation test was only performed from 4 to 6.5 GHz. Measured and simulated peak gain and the AR (Phi = 0 deg, Theta = 0 deg) of the proposed CP FPCA with metal strips are shown in Fig. 23. The test results show that the AR of the antenna is less than 3dB in the range of 4-6.5 GHz, which is consistent with the simulation results in the overall trend. The AR deteriorates a little at a lower frequency band but it is overall less than 3 dB. The antenna peak gain is 14.5 dB and the 3 dB gain bandwidth is 43.2% (4.12-6.39GHz). The far-field radiation patterns at different frequencies, i.e. 4, 5, 6, and 6.5 GHz, for the two principal E and H planes are illustrated in Fig. 24. The proposed antenna exhibits right-hand circular polarization (RHCP) in the broad-side direction.

The performance of the proposed CP FPCA is compared with other recently reported CP FPCA [7]–[11] which is summarized in Table 3. Some key parameters are listed, including 10 dB return loss bandwidth, 3 dB AR bandwidth, frequency band, substrate of FPC, height of FPC peak gain, and antenna volume. Table 3 indicates that our proposed antennas deliver both a broader AR bandwidth and a wide impedance bandwidth with a compact size. Compared with the previous research work, the proposed antenna CP bandwidth has obviously been improved.

IV. CONCLUSION

In this paper, a Tai Chi-shaped wideband CP antenna with 3D printed structure is proposed which utilizes a two-layer FPC structure to increase the gain and AR bandwidth. Simple metal strips are introduced on the basis of the FPC structure, which substantially increase the AR bandwidth. The peak gain is 14.5 dBic and the 3-dB gain bandwidth is 40.16% (4.2-6.3GHz). The proposed CP FPCA with metal strips exhibits not only a broad impedance bandwidth of 55.14% (3.82-7.01 GHz) but also a broad 3 dB AR bandwidth over 53.46% (4.07-7.04 GHz). The proposed antenna shows advantages in terms of substantially broadened impedance and AR bandwidth, high gain, and low fabrication cost. The proposed method of introducing some metal strips to enhance the AR bandwidth is very simple and effective, which could be applied in different frequency ranges. The proposed antenna could be used in many different application scenarios, such as the in-door UWB positioning system, 5G WLAN, RFID systems, and 5G base stations.

REFERENCES

[1] Q.-Y. Guo and H. Wong, "Wideband and high-gain Fabry–Pérot cavity antenna with switched beams for millimeter-wave applications," *IEEE Trans. Antennas Propag.*, vol. 67, no. 7, pp. 4339–4347, Jul. 2019.

[2] W. Lee, J. Kim, and Y. J. Yoon, "Compact two-layer rotman lens-fed microstrip antenna array at 24 GHz," *IEEE Trans. Antennas Propag.*, vol. 59, no. 2, pp. 460–466, Feb. 2011.

[3] Y. J. Cheng, W. Hong, and K. Wu, "Millimeter-wave substrate integrated waveguide multibeam antenna based on the parabolic reflector principle," *IEEE Trans. Antennas Propag.*, vol. 56, no. 9, pp. 3055–3058, Sep. 2008.

[4] X. Dong, H. Wang, Y. Liu, and L. Zhang, "A circularly polarized magneto-electric dipole leaky wave antenna with broadside radiation based on SIW technology," in *Proc. IEEE Int. Symp. Antennas Propag. USNC/URSI Nat. Radio Sci. Meeting*, Boston, MA, USA, Jul. 2018, pp. 1835–1836.

[5] G. Yang, J. Li, D. Wei, and R. Xu, "Study on wide-angle scanning linear phased array antenna," *IEEE Trans. Antennas Propag.*, vol. 66, no. 1, pp. 450–455, Jan. 2018.

[6] C. C. Counselman, "Multipath-rejecting GPS antennas," *Proc. IEEE*, vol. 87, no. 1, pp. 86–91, Jan. 1999.

[7] E. Brookner, W. Hall, and R. Westlake, "Faraday loss for L-band radar and communications systems," *IEEE Trans. Aerosp. Electron. Syst.*, vol. AES-21, no. 4, pp. 459–469, Jul. 1985.

[8] N. Hussain, M.-J. Jeong, J. Park, and N. Kim, "A broadband circularly polarized Fabry–Pérot resonant antenna using a single-layered PRS for 5G MIMO applications," *IEEE Access*, vol. 7, pp. 42897–42907, 2019.
[9] F. Wu and K. M. Luk, "Circular polarization and reconfigurability of Fabry–Pérot resonator antenna through metamaterial-loaded cavity," *IEEE Trans. Antennas Propag.*, vol. 67, no. 4, pp. 2196–2208, Apr. 2019.
[10] W. Cao, X. Lv, Q. Wang, Y. Zhao, and X. Yang, "Wideband circularly polarized Fabry–Pérot resonator antenna in Ku-band," *IEEE IEEE Antennas Wireless Propag. Lett.*, vol. 18, no. 4, pp. 586–590, Apr. 2019.
[11] N. Nguyen-Trong, H. H. Tran, T. K. Nguyen, and A. M. Abbosh, "A compact wideband circular polarized Fabry–Pérot antenna using resonance structure of thin dielectric slabs," *IEEE Access*, vol. 6, pp. 56333–56339, 2018.
[12] S. D. Jagtap, R. K. Gupta, N. Chaskar, S. U. Kharche, and R. Thakare, "Gain and bandwidth enhancement of circularly polarized MSA using PRS and AMC layers," *Prog. Electromagn. Res. C*, vol. 87, pp. 107–118, 2018.
[13] D. Comite, P. Baccarelli, P. Burghignoli, and A. Galli, "Omnidirectional 2-D leaky-wave antennas with reconfigurable polarization," *IEEE Antennas Wireless Propag. Lett.*, vol. 16, pp. 2354–2357, 2017.
[14] J. Huang, "A technique for an array to generate circular polarization with linearly polarized elements," *IEEE Trans. Antennas Propag.*, vol. 34, no. 9, pp. 1113–1124, Sep. 1986.
[15] A. Foroozesh and L. Shafai, "Investigation into the effects of the patch-type FSS superstrate on the high-gain cavity resonance antenna design," *IEEE Trans. Antennas Propag.*, vol. 58, no. 2, pp. 258–270, Feb. 2010.
[16] G. V. Trentini, "Partially reflecting sheet arrays," *IRE Trans. Antennas Propag.*, vol. 4, no. 4, pp. 666–671, Oct. 1956.
[17] D. R. Jackson and A. A. Oliner, "A leaky-wave analysis of the high-gain printed antenna configuration," *IEEE Trans. Antennas Propag.*, vol. 36, no. 7, pp. 905–910, Jul. 1988.
[18] H. Yang and N. Alexopoulos, "Gain enhancement methods for printed circuit antennas through multiple superstrates," *IEEE Trans. Antennas Propag.*, vol. 35, no. 7, pp. 860–863, Jul. 1987.
[19] T. H. Vu, K. Mahdjoubi, A.-C. Tarot, and S. Collardey, "Bandwidth enlargement of plannar EBG antennas," in *Proc. LAPC (Loughborough Antennas Propag. Conf.)*, Loughborough, U.K., 2007, pp. 152–153.
[20] B. Yen Toh, R. Cahill, and V. F. Fusco, "Understanding and measuring circular polarization," *IEEE Trans. Educ.*, vol. 46, no. 3, pp. 313–318, Aug. 2003.
[21] D. Lerner, "A wave polarization converter for circular polarization," *IEEE Trans. Antennas Propag.*, vol. AP-13, no. 1, pp. 3–7, Jan. 1965.
[22] N. Marcuvitz, *Waveguide Handbook* (Electromagnetic Waves), vol. 10. New York, NY, USA: McGraw-Hill, 1951, pp. 29–33 and 280–289.

YANG CHENG (Student Member, IEEE) received the B.S. degree in electrical engineering from the University of Electronic Science and Technology of China (UESTC), Chengdu, China, in 2018, where he is currently pursuing the M.S. degree. His research interests include miniaturized antennas, planar antennas, and microwave devices for handset and base station applications.

YUANDAN DONG (Senior Member, IEEE) received the B.S. and M.S. degrees from the Department of Radio Engineering, Southeast University, Nanjing, China, in 2006 and 2008, respectively, and the Ph.D. degree from the Department of Electrical Engineering, University of California at Los Angeles (UCLA), in 2012.

From September 2008 to June 2012, he was a Graduate Student Researcher with the Microwave Electronics Laboratory, UCLA. From September 2012 to February 2016, he was worked as a Senior Engineer with the R&D Hardware Department, Qualcomm in San Diego. From February 2016 to December 2017, he was worked as a Staff Engineer with Universal Electronics Inc., Santa Ana, CA, USA. Since December 2017, he has been a Full Professor with the University of Electronic Science and Technology of China (UESTC). He has authored more than 60 journal and conference papers. His research interests include the characterization and development of RF and microwave components, circuits, antennas, acoustic-wave filters, and metamaterials. He is also serving as a Reviewer for several IEEE and IET journals, including the IEEE TRANSACTIONS ON MICROWAVE THEORY AND TECHNIQUES and the IEEE TRANSACTION ON ANTENNAS AND PROPAGATION. He was a recipient of the Best Student Paper Award from the 2010 Asia Pacific Microwave Conference held in Yokohama, Japan. He was also a recipient of the Distinguished Expert Presented by Sichuan Province and by the China Government, respectively. He was also a recipient of the High Level Innovative and Entrepreneurial Talent presented by Jiangsu Province.